

Variable Star Candidates in an ACS Field of M31

Benjamin F. Williams¹

ABSTRACT

A search for variable stars is performed using two epochs of Hubble Space Telescope (HST) Advanced Camera for Surveys (ACS) imaging data for a 9.28 square arcminute portion of M31. This data set reveals 254 sources that vary by at least 4σ between epochs. The positions and 2-epoch *B*-band (equivalent) photometry of these sources are presented. The photometry suggests that this catalog includes most of the RR Lyrae population of this portion of M31.

1. Introduction

The proximity of M31 has made it one of the most important galaxies for the study of variable stars. Cepheid studies date back more than 40 years (Baade & Swope 1963, 1965), and continue in recent years. For example, the DIRECT project has found hundreds of Cepheids, as well as eclipsing binaries in M31 (Kaluzny et al. 1998, 1999; Stanek et al. 1998, 1999; Mochejska et al. 1999; Bonanos et al. 2003; Joshi et al. 2003) to exploit the fact that M31 provides a crucial step in the extragalactic distance ladder.

Variability studies of M31 have become diverse over last the few decades. These efforts include surveys for classical novae (Rosino 1973; Rosino et al. 1989; Sharov & Alksnis 1991; Shafter & Irby 2001; Filippenko & Chornock 2002; Rector 2003; Darnley et al. 2004, and many others) and most recently, efforts to detect microlensing events (Crotts 1992; Crotts & Tomaney 1996; Ansari et al. 1997; Aurière et al. 2001; Kerins et al. 2001; Paulin-Henriksson et al. 2003; Calchi Novati et al. 2002, 2003; Kerins et al. 2003; de Jong et al. 2004).

The data from these extensive surveys for Cepheids, novae, and microlensing events has provided large catalogs of the bright variable stars in M31. The POINT-AGAPE collaboration has published a catalog with 35,414 variable stars to an *r* magnitude limit ~ 23 in 0.6 square degrees, not overlapping with the field discussed herein. This wide-field study determined that the variable star distribution is highly asymmetric (An et al. 2004). The

¹Harvard-Smithsonian Center for Astrophysics, 60 Garden Street, Cambridge, MA 02138; williams@head-cfa.harvard.edu

DIRECT project (see references above) cataloged hundreds of variable stars in 5 fields, each 120 square arcmin. My ACS field overlaps with their field M31D (Kaluzny et al. 1999), but the ACS data is several magnitudes deeper. Joshi et al. (2003) cataloged hundreds more variable stars in a 170 square arcmin field, and Mould et al. (2004) has completed a large survey for bright, long period variables in M31, cataloging nearly 2000. Their fields also overlap with my ACS field, but are not as deep as my ACS data.

The deepest ground-based searches for M31 variables to date have been those of Dolphin et al. (2004) and Pritchett & van den Bergh (1987). These surveys were sufficiently deep to study the RR Lyrae population. Dolphin et al. (2004) cataloged 37 variable stars in a search for RR Lyrae stars in the M31 halo. They found 24 RR Lyrae stars, whose magnitudes suggest that they are metal poor. Their analysis suggested an RR Lyrae density of ~ 1 arcmin $^{-2}$. These results contrasted those of Pritchett & van den Bergh (1987), who found 30 RR Lyrae stars in a 7 square arcminute field. Their completeness analysis implied ~ 17 RR Lyrae stars arcmin $^{-2}$. The deepest search to date is that of Brown et al. (2004), who have used *HST*/ACS to search for variables in M31, finding 55 RR Lyrae stars, implying a density of ≥ 4 arcmin $^{-2}$ in their field.

Herein, I report the results of a search for variables in M31 with ACS imaging. Section 2 describes the 2-epoch ACS data set used and the analysis performed. Section 3 gives the results of the analysis. Section 4 discusses the types of variable stars these are most likely to be, and §5 summarizes the conclusions.

2. Data

The data used for this project were originally obtained as part of a program to find the optical counterparts for X-ray novae in M31 (Williams et al. 2005). I obtained two sets of *HST* ACS data, one observed at UT 21:35 on 03-Dec-2003 and one observed at UT 16:38 on 01-Mar-2004. Each of these were pointed at R.A.=00:44:07, Dec.=41:12:19.5. The observations had orientations of 71.75 deg and 32.73 deg respectively. Both observations were taken using the standard ACS box 4-point dither pattern to allow the final data to be drizzled to recover the highest possible spatial resolution. All exposures were taken through the F435W filter. The total exposure times were 2200 seconds for each data set. The 9.275 arcmin 2 overlapping region of the two ACS images is outlined on a wide-field H α image of M31 in Figure 1.

2.1. Image Processing, Alignment and Subtraction

I aligned and drizzled each set of 4 images into high-resolution ($0.025''$ pixel $^{-1}$) images using the PyRAF² task *multidrizzle*,³ which has been optimized to process ACS imaging data. The task removes the cosmic ray events and geometric distortions, and it drizzles the dithered frames together into one final photometric image with pixel values in units of counts per second.

I aligned the final photometric ACS images with the coordinate system of the Local Group Survey (LGS; Massey et al. 2001) by applying the IRAF⁴ task *cemap* to the centroids of stars and globular clusters common to the ACS and LGS images. The LGS images have an assigned J2000 (FK5) world coordinate system accurate to $\sim 0.25''$, and they provided the standard coordinate system to which I aligned all of the data for this project. The alignment errors measured by *cemap* were $\sim 0.025''$, or one pixel in the drizzled images.

In order to produce ACS images from each epoch with aligned pixel orientations, I used the IRAF tasks *geomap* and *geotran* to map and transform the images so that the pixels were aligned in the North up, East left orientation. I used the same objects to transform both epochs to the new pixel orientation. This technique resulted in images with identical pixel orientations and aligned to an accuracy of 0.2 pixels.

Since the aligned data from both epochs had the same exposure times, were taken through the same filter, and were processed with identical techniques, the images were subtracted directly to search for residual sources that were due to their brightness changing between the two observations.

2.2. Search Technique

Most bright stars left some form of residual in the difference image due to the different roll angles of the two fields and different locations of the stars on the ACS detector. Although these residuals had a distinctive appearance that did not resemble a point source, they

²PyRAF is a product of the Space Telescope Science Institute, which is operated by AURA for NASA.

³multidrizzle is a product of the Space Telescope Science Institute, which is operated by AURA for NASA.
<http://stsdas.stsci.edu/pydrizzle/multidrizzle>

⁴IRAF is distributed by the National Optical Astronomy Observatory, which is operated by the Association of Universities for Research in Astronomy, Inc., under cooperative agreement with the National Science Foundation.

severely hampered automated searches of the difference image by producing an overwhelming number of false variability detections. As these images are very large (10^8 pixels), automated search routines proved slow and inefficient. Preliminary visual searches of the difference image greatly reduced the number of false variability detections, increasing the efficiency and reliability of the search, with 93% of the visual candidates passing the remaining tests for variability between the two epochs (see § 2.3).

The difference image was searched twice visually for variable candidates. All residuals that appeared as point spread functions were flagged. The first search was performed with the contrast of the image set so that sources that were brighter during the first epoch appeared as black spots. The second search was performed with the inverse contrast setting, in order to find objects that were brighter in the second epoch. Examples of a variable that became brighter and one that became fainter, including their appearances at both contrast settings, are shown in Figure 2.

The searches resulted in 141 candidates that were brighter in the first epoch and 133 candidates that were brighter in the second epoch. The fact that these numbers were within \sqrt{N} of one another was encouraging that the search technique was not introducing any large bias to the sample.

The candidates' final positions were determined with the IRAF task *imcentroid*. Positions of the objects were measured with data from the epoch in which the object appeared brighter. Two objects did not provide reliable centroids, suggesting that they were not strong detections and/or not point sources. These candidates were removed, leaving a final list of 272 variable star candidates to be measured.

2.3. Photometry

Aperture photometry was performed at the *imcentroid* position for each candidate using the IRAF task *phot*. The aperture radius was $0.15''$, and the annulus used to measure the sky brightness was from $0.30''$ to $0.55''$. The photometry was performed identically for both epochs. These measurements yielded the ACS count rate for each candidate during each observation epoch.

The count rates measured from the ACS images were converted to VEGA magnitudes using the calibration provided in the ACS Data Handbook⁵. The VEGA magnitudes for the F435W filter is the ACS equivalent to the Johnson *B* magnitude. The final conversion

⁵http://www.stsci.edu/hst/acs/documents/handbooks/DataHandbookv2/ACS_longdhbcover.html

formula was:

$$m_B \approx F435W_{VEGA} = -2.5\log(r) + 25.76$$

where r is the count rate measured by $phot$. Sources with $B \sim 27.8$ were detected with 5σ significance. I took this to be the detection limit, only accepting detections brighter than this and assigning an upper-limit $B > 27.8$, to all non-detections.

The final B magnitudes from the second epoch were subtracted from those of the first, and the photometric errors were added in quadrature. No errors were assigned to non-detections.

All of the candidates whose magnitudes changed by four times the root-sum-square of their errors (or more) were included in the final catalog of variables given in Table 1. This requirement eliminated 3 candidates from the original list, reducing the catalog to 269 variable stars. Finally, for all cases of stars detected in only one epoch, the four dithered ACS exposures of the detection epoch were inspected to ensure that these detections were not cosmic-rays or artifacts from the image processing. Real stars were seen in all of the individual raw exposures, while cosmic rays and artifacts were not. These inspections found 15 of the variable candidates to be spurious: cases where *multidrizzle* had failed to properly reject a cosmic ray or artifact. The final catalog therefore contains 254 candidate variable stars.

The photometric properties of these variables are shown in Table 2 and Figure 3. They follow the expected pattern, as the smallest detected change in magnitude increases with increasing B magnitude. These statistics provide further confirmation that the search technique did not introduce any significant bias into the sample.

Comparisons of this catalog with the three previous overlapping surveys show that five variables from the Kaluzny et al. (1999) catalog and 6 variables from the Joshi et al. (2003) catalog lie within the 9.28 arcmin^2 variable-sensitive portion of my data set. Two of the six Joshi et al. (2003) survey variables were identified here as well, and all five of the Kaluzny et al. (1999) variables were identified here. Four of the Joshi et al. (2003) variables were not seen (V346, V351, V352 and V354), and five of the Mould et al. (2004) variables were not seen (44001, 44008, 44020, 44044, and 44045), possibly because of the differing bandpasses of their surveys which were completed in R and I . On the other hand, all of the variables of Kaluzny et al. (1999) were independently identified here. One source (DIRECT V4599 M31D) was culled from my catalog when *imcentroid* did not converge on its center in the ACS image, suggesting that it is blended or extended. The six previously-cataloged variables, including names and photometry from the previous identifications, are provided in Table 3.

3. Results

The final catalog of 254 variable stars in these 9.28 arcmin^2 of M31 is shown in Table 1. Names were determined using the an IAU-approved acronym (M31ACSV) followed by truncated J2000 coordinates in an IAU-approved format (JHHMMSS.s+DDMMSS). The variables range in brightness from $21.9 < B < 27.0$, and they show brightness changes $|\Delta B| > 0.15 \text{ mag}$. The distribution of brightnesses and brightness changes are shown in Figures 3-5 and discussed in § 4. One important note about Figure 3 is that, even though all of the brightness changes seen in this survey are lower limits, only those that were not detected in one of the two observations are marked as lower limits.

The density of variable stars in this small region of M31 is at least 27 arcmin^{-2} . This is about twice as high as that seen by Brown et al. (2004) in a field $51'$ from the nucleus. The higher density is not unexpected, as the field observed is only $17'$ from the nucleus.

This sample likely contains many types of variables, but only those that vary by more than 0.15 mag. Some could be novae, but as the observed nova rate for the entire Galaxy is only $\sim 25 \text{ yr}^{-1}$ (Romano et al. 1999), clearly the bulk of the variables in this tiny fraction of M31 are not novae. Most of these variables are likely pulsating stars and eclipsing binaries. Pulsating variables in this magnitude range that exhibit high-amplitude variability include Cepheids, irregular variables, Type II and Anomalous Cepheids, RR Lyrae stars, high-amplitude δ Scuti stars (HADS), and Long Period Variables (LPVs; Gautschy & Saio 1996 and references therein). Well-sampled lightcurves will be needed to obtain reliable source classifications; however, assuming eclipsing binaries randomly populate the $|\Delta B| - B$ plane in low numbers, the relative numbers of some types of variable stars can be roughly estimated based on the $|\Delta B| - B$ diagram.

4. Discussion

The right panel of Figure 3 shows the $|\Delta B| - B$ plane divided into areas, each labeled with the type of variable star that most likely occupies it. Eclipsing binaries can lie anywhere in the $|\Delta B| - B$ plane. While these labeled areas are not reliable classifications, they provide a guide regarding where certain types of stars most likely fall in the figure. This section discusses the justification of these labels.

4.1. The Brightest Candidates

The six stars that reached $B < 23$ (J004400.3+411309, J004401.0+411132, J004402.5+411137, J004404.0+411353, J004408.0+411243 and J004408.4+411347) would be easily detectable in ground based images. Four of these stars (J004401.0+411132, J004404.0+411353, J004408.0+411243 and J004408.4+411347) were previously cataloged (see Table 3). The other two (J004400.3+411309 and J004402.5+411137) changed in brightness by less than 0.5 mag, which could be difficult to detect in ground-based photometry. Fainter variables would be quite difficult to detect in ground-based surveys because of the effects of crowding. The two other variables that were previously cataloged were observed in the R and I bands, where they have $m < 21$ (Joshi et al. 2003).

Those stars with $B_{bright} < 24.5$ are brighter than RR Lyrae stars in M31. These stars may be Type II Cepheids and/or Anomalous Cepheids (Wallerstein & Cox 1984; Wallerstein 2002; Marconi et al. 2004). These types of Cepheids are typically fainter than Type I Cepheids and brighter than RR Lyrae stars. Their amplitudes of variation are similar to RR Lyrae stars. The catalog contains 16 newly-discovered variable candidates that may have these characteristics ($23 < B_{bright} < 24.5$; $|\Delta B| < 1.5$). Although some of these stars could be bright LPVs, the magnitudes of these stars in this study make them the best Type II and Anomalous Cepheid candidates in the catalog.

4.2. Fainter Candidates

The histogram in Figure 4 exhibits a clear peak at $B \approx 25.5$. The density of variables appears to increase sharply at magnitudes fainter than $B \approx 24.5$ or $M_B \approx -0.4$. The density increases from $2.2 \text{ arcmin}^{-2} \text{ mag}^{-1}$ to $14.6 \text{ arcmin}^{-2} \text{ mag}^{-1}$ as B goes from 24 to 25. This increase is in proportion to the increase in the stellar density, which goes from $220 \text{ arcmin}^{-2} \text{ mag}^{-1}$ to $1210 \text{ arcmin}^{-2} \text{ mag}^{-1}$ over the same magnitude range. These numbers show that at least $\sim 1\%$ of the stars in this region of M31 with $B < 25.5$ are variable.

Some of the decrease in the number of variables found at magnitudes fainter than $B \approx 26$ is due to the limitations of the search technique at those magnitudes on this data set. Variables fainter than $B \approx 26$ are more likely to be mistaken for noise in the difference image, and as can be seen in Figure 3, stars with $B_{bright} > 26$ must change in brightness by > 0.5 mag to pass all of the variability criteria.

Although the peak in the brightness distribution can be explained by completeness effects, it is interesting that the peak is at $B \approx 25.5$. With a distance modulus of 24.47 and a typical extinction of $A_B = 0.4$ mag (Williams 2003), this brightness corresponds

to $M_B \approx 0.6$, typical for RR Lyrae stars with a range of metallicities according to the luminosity–metallicity relation (Chaboyer 1999; Cacciari & Clementini 2003). Allowing for the possibility that RR Lyrae stars in this field may cover a range in metallicities from $-2 \lesssim [\text{Fe}/\text{H}] \lesssim 0$ (including disk and halo populations), they may cover a range in luminosities from $0.3 < \langle M_V \rangle < 1.0$. The errors in the slope and zero point of the luminosity–metallicity relation were included in the determination of this range. In addition, RR Lyrae stars could have amplitudes as great as $\Delta B \approx 1.5$ (e.g., AQ Lyr; Castellani et al. 1998).

The space density of RR Lyrae stars in the solar vicinity is 6 kpc^{-3} (Amrose & Mckay 2001). With an inclination of 77 degrees, assuming a disk thickness of 1 kpc, 1 arcmin^2 of M31 corresponds to $\sim 0.2 \text{ kpc}^3$. Therefore, 1–2 RR Lyrae arcmin^{-2} from the M31 disk should be seen. If the RR Lyrae density of the Brown et al. (2004) field ($\sim 4 \text{ arcmin}^{-2}$) is added to this disk estimate, RR Lyrae stars should account for *more than* 50–60 of the variables in this catalog, as the present field is in a more dense region of M31 than the Brown et al. (2004) field. Assuming foreground extinction $A_B \approx 0.4$ and a range of $B - V$ colors from 0 to 0.5, RR Lyrae stars are likely to occupy the $|\Delta B| < 1.5$ and $24.5 \lesssim B_{bright} \lesssim 26.5$ portion of Figure 3. This section of the plot contains 175 stars, suggesting that the catalog includes a large fraction of the RR Lyrae stars in this region of M31.

In addition, this section of the plot may contain some faint Type II and Anomalous Cepheid stars, as well as bright HADS. HADS are distinct from RR Lyrae stars in that they are typically Population I and have shorter periods (see Gautschy & Saio 1996; Rodríguez et al. 2000 and references therein). These stars range in spectral type from A2–F0 ($1.3 < M_B < 3.0$), and can be as much as 2 magnitudes brighter than the main sequence (Garcia et al. 1995). Therefore bright HADS can overlap with the magnitude range covered by RR Lyrae stars, adding to the number of potential RR Lyrae stars in the catalog.

Finally, many of these variable sources could be LPVs or eclipsing binaries. LPVs likely account for a large number of the variables in the catalog, as Brown et al. (2004) found them to be common in their ACS field. These stars have $1 \lesssim B - V \lesssim 3$, can exhibit B magnitude variations of greater than 4 magnitudes, and have maximum luminosities of $-1 \lesssim M_B \lesssim 2$ (Celis S. 1986; de Laverny et al. 1997). With only 2 epochs of photometry, LPVs are likely present at all B_{bright} magnitudes fainter than ~ 24 , and the highest amplitude variables, with $|\Delta B| > 1.5$ mag, are the most likely to be LPVs or eclipsing binaries.

5. Conclusions

The 2-epoch $F435W$ -band (B equivalent) photometric properties of an *HST* ACS field in M31 have been measured, resulting in a catalog of the positions and magnitudes of 254 likely variable stars in 9.28 arcmin^2 . This catalog provides a starting point from which to study the variable star population of this region of M31 at RR Lyrae magnitudes.

With only 2 epochs of photometry, the variable sources cannot be individually classified; however, with just two epochs there appears to be a high density ($>27 \text{ arcmin}^{-2}$) of variable stars in M31. Four of the brightest variables are previously known periodic variables, including one Cepheid. The other bright variables could be bright irregular, periodic, eclipsing binary, Type II Cepheid, or anomalous Cepheid stars.

A comparison of the density of variables in this catalog at RR Lyrae magnitudes with the density of such stars in the Galaxy and in previous M31 surveys suggests that this catalog includes most of the RR Lyrae stars in this portion of M31. Additionally, the catalog likely includes many LPVs, along with some high-amplitude δ Scuti stars and eclipsing binaries.

I thank Michael Garcia for his many helpful comments. Support for this work was provided by NASA through grant G0-9087 from the Space Telescope Science Institute and through grant GO-3103X from the *Chandra* X-Ray Center.

REFERENCES

Amrose, S., & Mckay, T. 2001, ApJ, 560, L151

An, J. H., et al. 2004, MNRAS, 351, 1071

Ansari, R., et al. 1997, A&A, 324, 843

Aurière, M., et al. 2001, ApJ, 553, L137

Baade, W., & Swope, H. H. 1963, AJ, 68, 435

Baade, W., & Swope, H. H. 1965, AJ, 70, 212

Bonanos, A. Z., Stanek, K. Z., Sasselov, D. D., Mochejska, B. J., Macri, L. M., & Kaluzny, J. 2003, AJ, 126, 175

Brown, T. M., Ferguson, H. C., Smith, E., Kimble, R. A., Sweigart, A. V., Renzini, A., & Rich, R. M. 2004, AJ, 127, 2738

Cacciari, C., & Clementini, G. 2003, Lecture Notes in Physics, Berlin Springer Verlag, 635, 105

Calchi Novati, S., et al. 2002, A&A, 381, 848

Calchi Novati, S., Jetzer, P., Scarpetta, G., Giraud-Héraud, Y., Kaplan, J., Paulin-Henriksson, S., & Gould, A. 2003, A&A, 405, 851

Castellani, V., di Paolantonio, A., Piersimoni, A. M., & Ripepi, V. 1998, A&A, 333, 918

Celis S., L. 1986, AJ, 91, 405

Chaboyer, B. 1999, in ASSL Vol. 237: Post-Hipparcos cosmic candles, 111

Crotts, A. P. S. 1992, ApJ, 399, L43

Crotts, A. P. S., & Tomaney, A. B. 1996, ApJ, 473, L87

Darnley, M. J., et al. 2004, MNRAS, 262

de Jong, J. T. A., et al. 2004, A&A, 417, 461

de Laverny, P., Geoffray, H., Jorda, L., & Kopp, M. 1997, A&AS, 122, 415

Dolphin, A. E., Saha, A., Olszewski, E. W., Thim, F., Skillman, E. D., Gallagher, J. S., & Hoessel, J. 2004, AJ, 127, 875

Filippenko, A. V., & Chornock, R. 2002, IAU Circ., 7825, 3

Garcia, J. R., et al. 1995, A&AS, 109, 201

Gautschy, A., & Saio, H. 1996, ARA&A, 34, 551

Joshi, Y. C., Pandey, A. K., Narasimha, D., Sagar, R., & Giraud-Héraud, Y. 2003, A&A, 402, 113

Kaluzny, J., Mochejska, B. J., Stanek, K. Z., Krockenberger, M., Sasselov, D. D., Tonry, J. L., & Mateo, M. 1999, AJ, 118, 346

Kaluzny, J., Stanek, K. Z., Krockenberger, M., Sasselov, D. D., Tonry, J. L., & Mateo, M. 1998, AJ, 115, 1016

Kerins, E., et al. 2003, ApJ, 598, 993

Kerins, E., et al. 2001, MNRAS, 323, 13

Marconi, M., Fiorentino, G., & Caputo, F. 2004, *A&A*, 417, 1101

Massey, P., Hodge, P. W., Holmes, S., Jacoby, G., King, N. L., Olsen, K., Saha, A., & Smith, C. 2001, in American Astronomical Society Meeting, Vol. 199, 13005

Mochejska, B. J., Kaluzny, J., Stanek, K. Z., Krockenberger, M., & Sasselov, D. D. 1999, *AJ*, 118, 2211

Mould, J., Saha, A., & Hughes, S. 2004, *ApJS*, 154, 623

Paulin-Henriksson, S., et al. 2003, *A&A*, 405, 15

Pritchett, C. J., & van den Bergh, S. 1987, *ApJ*, 316, 517

Rector, T. A. 2003, *IAU Circ.*, 8210, 4

Rodríguez, E., López-González, M. J., & López de Coca, P. 2000, *A&AS*, 144, 469

Romano, D., Matteucci, F., Molaro, P., & Bonifacio, P. 1999, *A&A*, 352, 117

Rosino, L. 1973, *A&AS*, 9, 347

Rosino, L., Capaccioli, M., D’Onofrio, M., & della Valle, M. 1989, *AJ*, 97, 83

Shafter, A. W., & Irby, B. K. 2001, *ApJ*, 563, 749

Sharov, A. S., & Alksnis, A. 1991, *Ap&SS*, 180, 273

Stanek, K. Z., Kaluzny, J., Krockenberger, M., Sasselov, D. D., Tonry, J. L., & Mateo, M. 1998, *AJ*, 115, 1894

Stanek, K. Z., Kaluzny, J., Krockenberger, M., Sasselov, D. D., Tonry, J. L., & Mateo, M. 1999, *AJ*, 117, 2810

Wallerstein, G. 2002, *PASP*, 114, 689

Wallerstein, G., & Cox, A. N. 1984, *PASP*, 96, 677

Williams, B. F. 2003, *AJ*, 126, 1312

Williams, B. F., Garcia, M. R., Kong, A. K. H., Primini, F. A., & Murray, S. S. 2005, *ApJ*, submitted

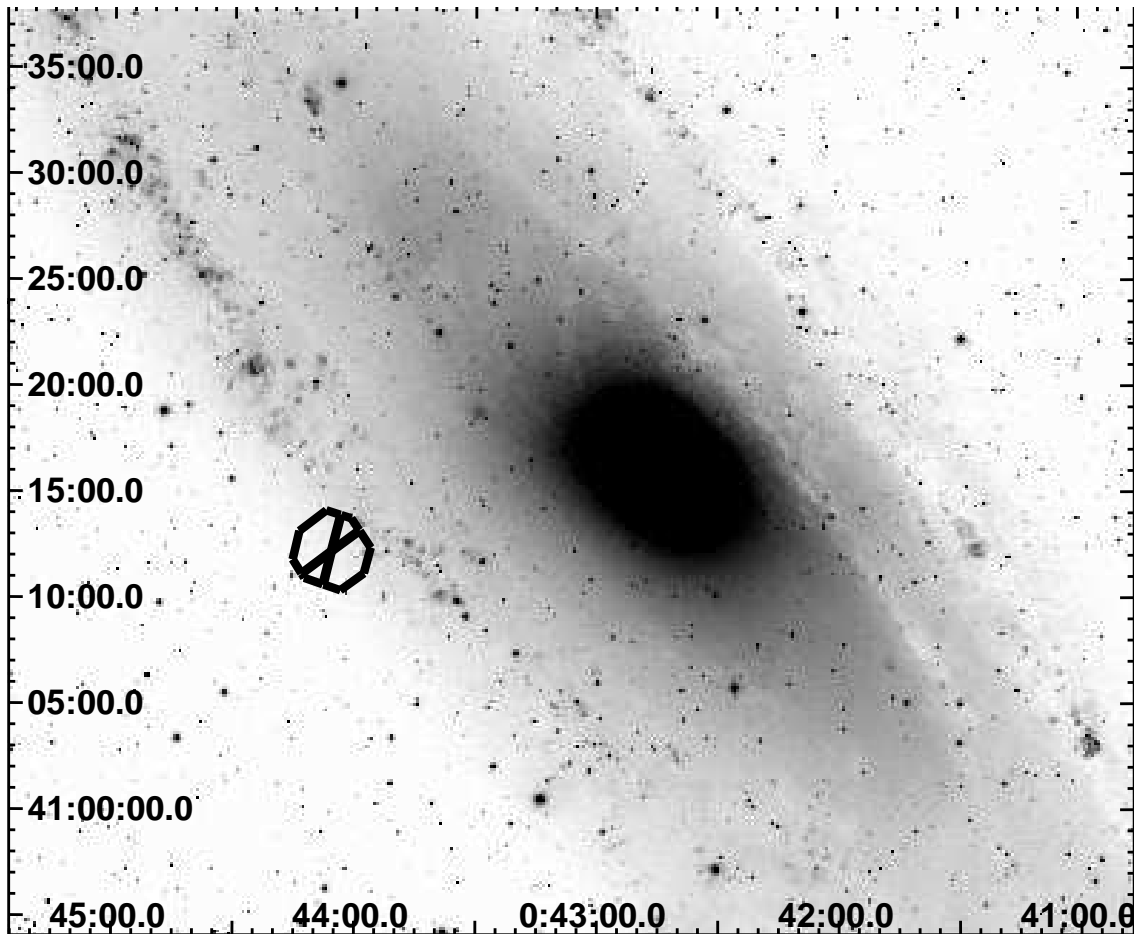


Fig. 1.— An H α image of a portion of M31 is shown. The polygon drawn in black at 00:44.1, 41:12.1 outlines the area where the ACS data set was sensitive to variable sources. The cross inside the polygon shows the location of the chip gap in each of the 2 epochs.

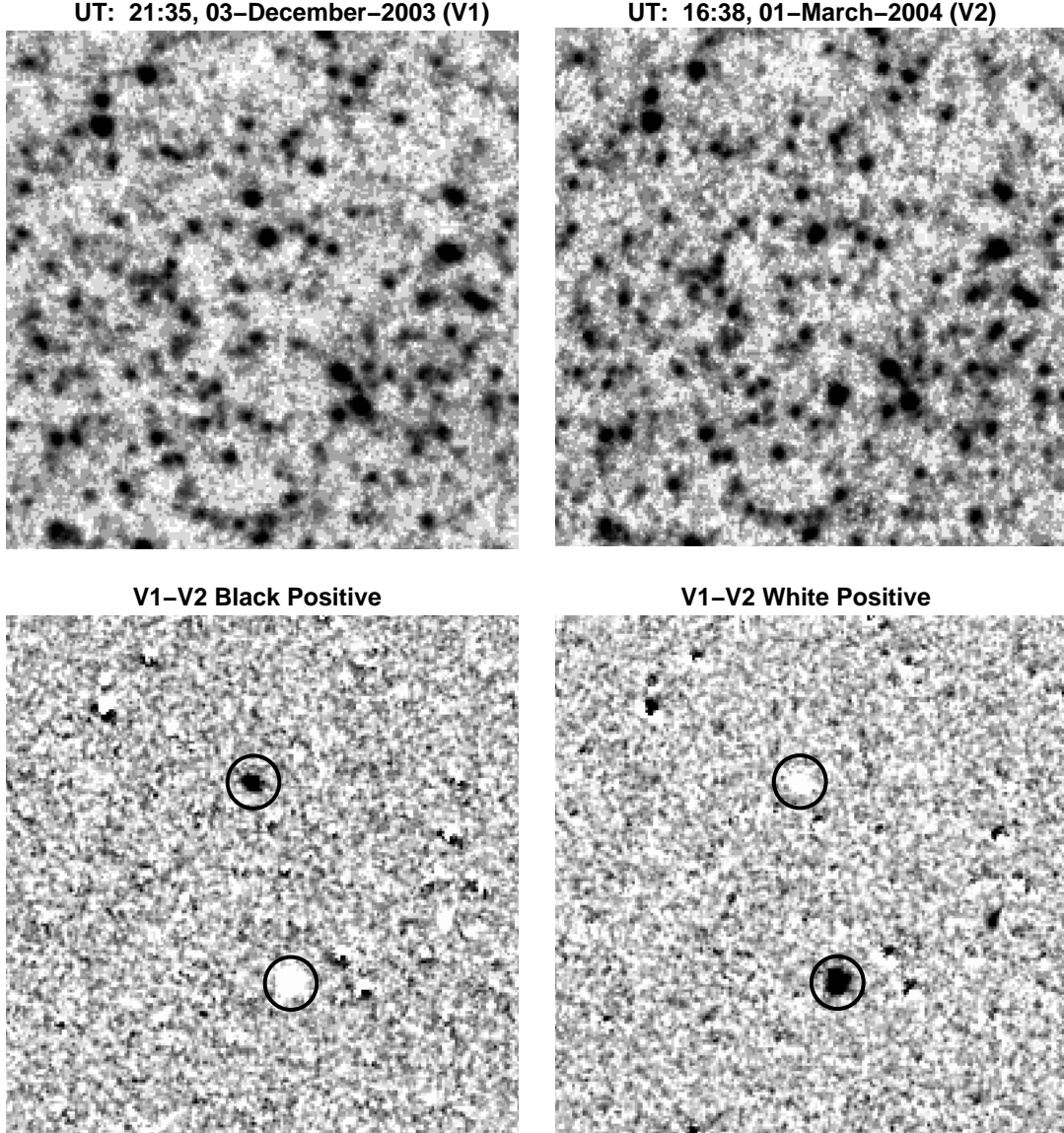


Fig. 2.— Example images from the variable search. *Upper left:* A $5'' \times 5''$ portion of the first ACS image of the field, taken 03–December–2003, designated as V1; black is positive. *Upper right:* A $5'' \times 5''$ portion of the second ACS image of the field, taken 01–March–2004, designated as V2; black is positive. *Lower left:* The difference image, V1–V2, displayed so that black is positive, revealing variables like M31ACSV J004407.7+411333 (marked with the upper black circle), that were brighter during the first exposure. *Lower right:* The difference image, V1–V2, displayed so that black is negative, revealing variables like M31ACSV J004407.7+411331 (marked with the lower black circle), that were brighter during the second exposure.

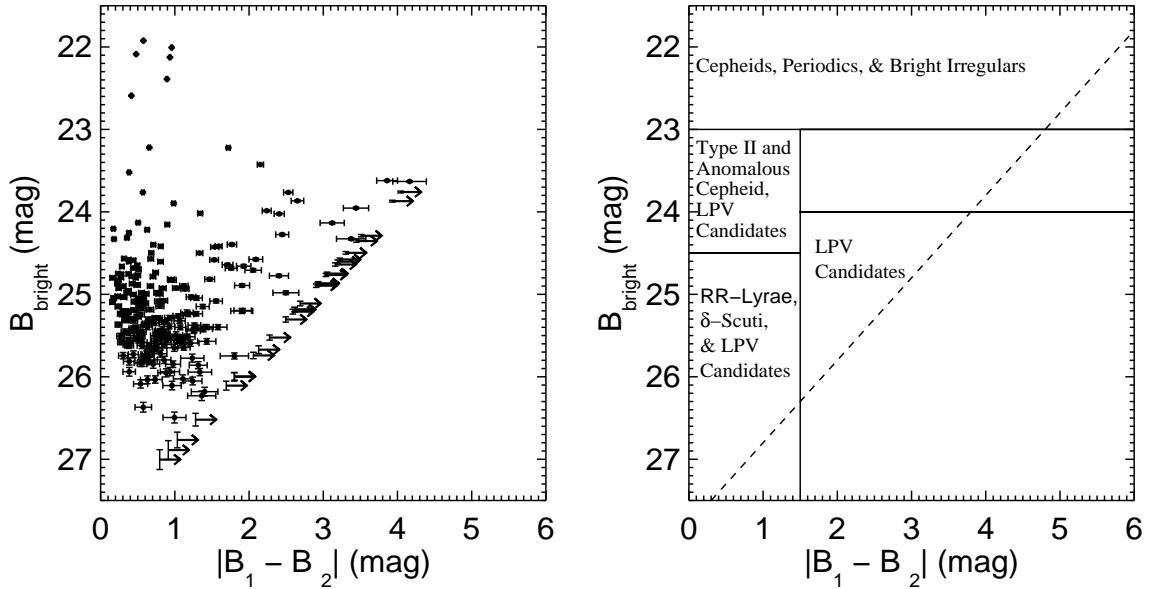


Fig. 3.— *Left:* The change in B magnitude observed is plotted against the brightest B magnitude observed. There is a dense grouping of sources with characteristics typical of RR Lyrae stars ($|\Delta B| \lesssim 1.5$ and $B \sim 25.5$). *Right:* The $|\Delta B| - B$ plane is shown divided into labeled areas (solid lines); each label gives the type of variable star that likely occupies that area of the $|\Delta B| - B$ plane. Eclipsing binaries could lie anywhere in the $|\Delta B| - B$ plane. The dashed line marks the magnitude limit of this survey.

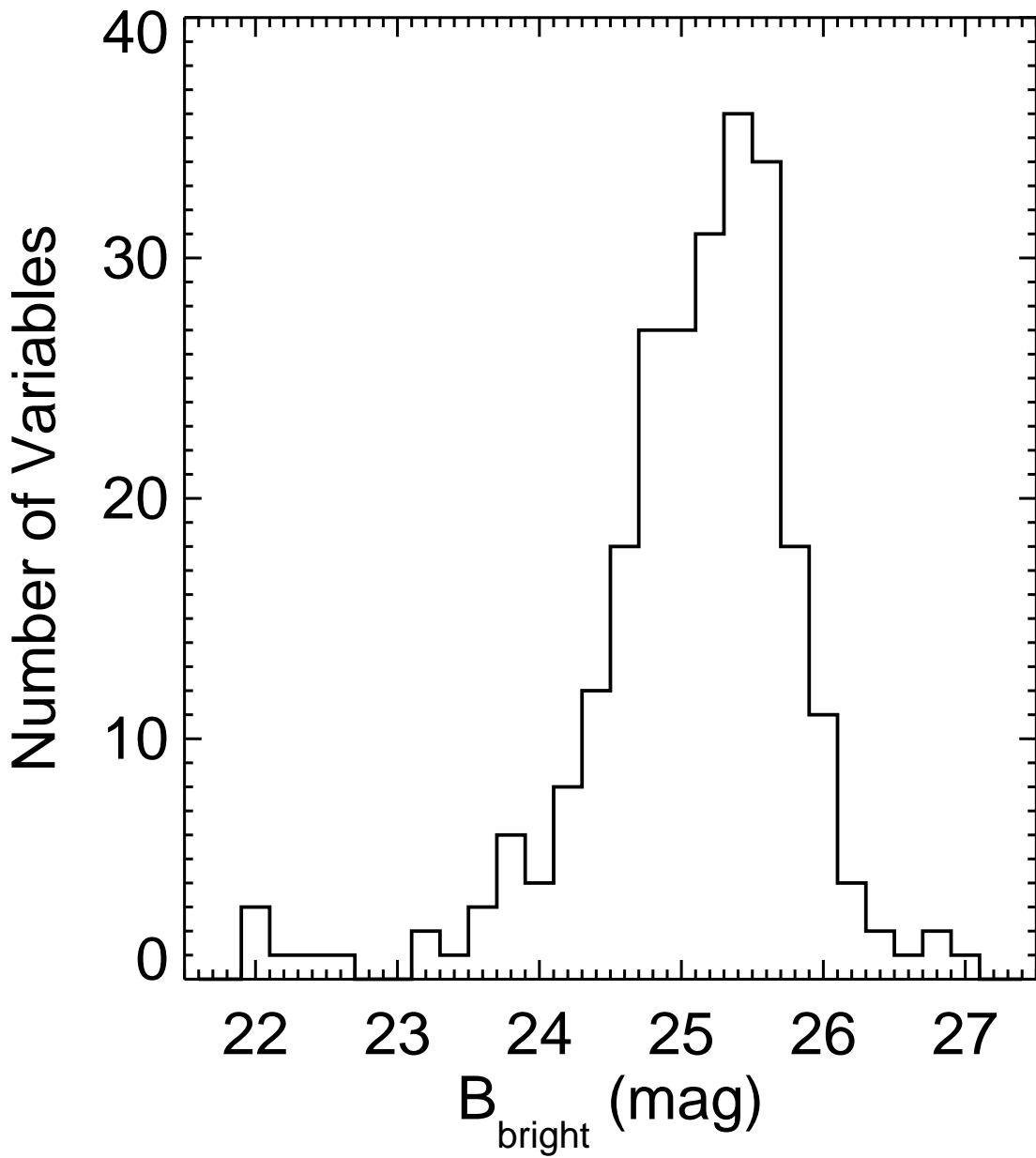


Fig. 4.— Histogram of the brightest B magnitude observed vs. the number of variables found. The search technique fails for variables that were not brighter than $B \sim 26$ in this data set.

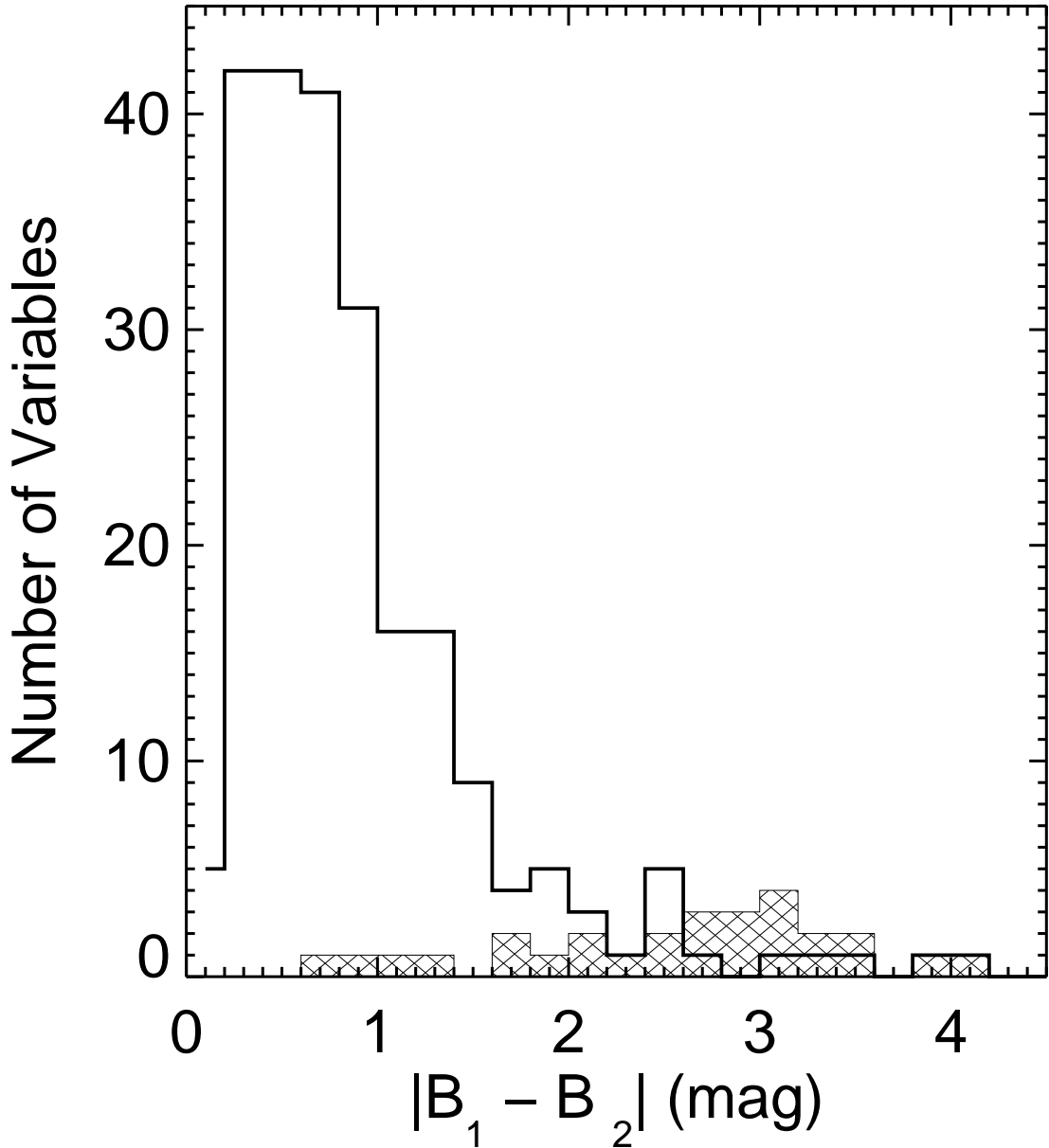


Fig. 5.— *Thick histogram*: the change in B magnitude observed vs. the number of variables found for the 226 variables detected in both epochs. A clear peak is seen at $|\Delta B| \sim 0.5$. *Hatched histogram*: the minimum change in B magnitude observed vs. the number of variables found for the 28 variables only detected in one epoch.

Table 1. Variable Stars in the ACS Field

Name (M31ACSV)	R.A. (J2000)	Dec. (J2000)	B_1^a	B_2^b	$B_1 - B_2$
J004357.5+411139	0:43:57.555	41:11:39.88	24.50±0.02	25.18±0.03	-0.68±0.03
J004357.6+411119	0:43:57.659	41:11:19.99	24.90±0.02	>27.8	<-2.90
J004357.7+411126	0:43:57.722	41:11:26.35	25.20±0.03	27.10±0.14	-1.90±0.15
J004357.9+411244	0:43:57.917	41:12:44.30	26.41±0.09	25.50±0.05	0.90±0.10
J004358.1+411250	0:43:58.194	41:12:50.15	23.22±0.01	23.88±0.01	-0.66±0.01
J004358.5+411238	0:43:58.516	41:12:38.30	26.53±0.08	25.72±0.04	0.81±0.09
J004358.6+411109	0:43:58.607	41:11:09.19	25.42±0.03	26.81±0.12	-1.39±0.12
J004358.6+411247	0:43:58.662	41:12:47.22	27.01±0.15	25.77±0.05	1.24±0.16
J004358.7+411211	0:43:58.701	41:12:11.11	24.60±0.02	25.41±0.03	-0.81±0.04
J004359.0+411159	0:43:59.063	41:11:59.47	26.25±0.06	25.48±0.03	0.77±0.07
J004359.3+411125	0:43:59.368	41:11:25.85	>27.8	23.76±0.01	>4.04
J004359.5+411059	0:43:59.529	41:10:59.95	>27.8	25.31±0.03	>2.49
J004359.6+411221	0:43:59.613	41:12:21.77	24.33±0.01	27.70±0.20	-3.38±0.20
J004359.8+411134	0:43:59.814	41:11:34.82	27.59±0.18	26.23±0.06	1.36±0.19
J004359.9+411126	0:43:59.964	41:11:26.22	25.93±0.05	25.08±0.02	0.85±0.05
J004400.0+411127	0:44:00.038	41:11:27.85	25.51±0.03	26.05±0.05	-0.54±0.06
J004400.1+411323	0:44:00.167	41:13:23.35	25.14±0.03	25.94±0.05	-0.80±0.05
J004400.3+411309	0:44:00.339	41:13:09.92	22.59±0.01	23.01±0.01	-0.41±0.01
J004400.5+411215	0:44:00.524	41:12:15.24	25.03±0.02	24.59±0.02	0.44±0.03
J004400.6+411107	0:44:00.677	41:11:07.30	23.76±0.01	26.29±0.06	-2.53±0.06
J004400.6+411239	0:44:00.683	41:12:39.68	25.61±0.03	25.37±0.03	0.24±0.04
J004400.6+411209	0:44:00.690	41:12:09.44	25.18±0.03	>27.8	<-2.62
J004400.7+411139	0:44:00.709	41:11:39.94	25.65±0.04	25.32±0.03	0.34±0.05
J004400.8+411243	0:44:00.804	41:12:43.30	25.03±0.03	25.35±0.03	-0.31±0.04
J004400.8+411047	0:44:00.826	41:10:47.15	26.07±0.05	24.94±0.02	1.14±0.05
J004400.8+411305	0:44:00.842	41:13:05.86	>27.8	27.00±0.12	>0.80
J004400.9+411117	0:44:00.914	41:11:17.11	25.52±0.03	>27.8	<-2.28
J004400.9+411204	0:44:00.985	41:12:04.37	24.29±0.01	>27.8	<-3.51
J004400.9+411324	0:44:00.985	41:13:24.04	25.05±0.02	25.56±0.04	-0.51±0.04
J004401.0+411342	0:44:01.025	41:13:42.44	>27.8	24.60±0.02	>3.20
J004401.0+411153	0:44:01.046	41:11:53.89	25.67±0.04	26.35±0.07	-0.68±0.08
J004401.0+411132	0:44:01.084	41:11:32.35	22.13±0.01	23.06±0.01	-0.93±0.01
J004401.2+411236	0:44:01.210	41:12:36.53	25.27±0.03	24.77±0.02	0.50±0.04
J004401.2+411233	0:44:01.241	41:12:33.02	24.90±0.02	25.57±0.04	-0.67±0.04
J004401.2+411344	0:44:01.289	41:13:44.36	25.19±0.03	25.65±0.04	-0.46±0.05
J004401.2+411042	0:44:01.294	41:10:42.94	25.20±0.02	27.11±0.12	-1.91±0.12
J004401.4+411057	0:44:01.465	41:10:57.60	25.49±0.03	24.79±0.02	0.71±0.04
J004401.5+411333	0:44:01.536	41:13:33.40	25.30±0.03	25.97±0.05	-0.66±0.06
J004401.5+411203	0:44:01.565	41:12:03.64	25.46±0.03	26.01±0.05	-0.56±0.06
J004401.5+411203	0:44:01.580	41:12:03.23	>27.8	26.11±0.05	>1.69
J004401.6+411154	0:44:01.603	41:11:54.88	24.80±0.02	25.07±0.03	-0.28±0.03
J004401.6+411327	0:44:01.663	41:13:27.35	25.66±0.04	26.41±0.07	-0.75±0.08
J004401.8+411107	0:44:01.825	41:11:07.85	25.57±0.03	27.00±0.12	-1.43±0.12
J004401.8+411133	0:44:01.861	41:11:33.61	26.39±0.07	25.75±0.05	0.63±0.09
J004402.0+411135	0:44:02.017	41:11:35.65	24.87±0.02	25.30±0.03	-0.43±0.04
J004402.0+411347	0:44:02.074	41:13:47.94	24.66±0.02	24.95±0.02	-0.29±0.03
J004402.0+411125	0:44:02.093	41:11:25.98	24.84±0.02	24.22±0.01	0.63±0.03
J004402.0+411215	0:44:02.093	41:12:15.05	25.22±0.03	25.05±0.03	0.18±0.04
J004402.1+411123	0:44:02.132	41:11:23.97	25.15±0.03	26.52±0.08	-1.38±0.09
J004402.1+411233	0:44:02.162	41:12:33.64	25.07±0.03	24.83±0.02	0.24±0.03
J004402.2+411342	0:44:02.282	41:13:42.00	25.22±0.03	26.39±0.08	-1.16±0.08
J004402.2+411346	0:44:02.288	41:13:46.06	24.90±0.02	25.21±0.03	-0.30±0.04
J004402.5+411137	0:44:02.512	41:11:37.10	22.57±0.01	22.09±0.00	0.48±0.01
J004402.5+411121	0:44:02.564	41:11:21.89	26.46±0.07	25.81±0.04	0.65±0.08

Table 1—Continued

Name (M31ACSV)	R.A. (J2000)	Dec. (J2000)	B_1^a	B_2^b	$B_1 - B_2$
J004402.6+411214	0:44:02.634	41:12:14.79	24.93±0.02	25.76±0.04	-0.84±0.05
J004402.6+411140	0:44:02.642	41:11:40.45	26.26±0.08	25.43±0.04	0.83±0.09
J004402.6+411148	0:44:02.650	41:11:48.66	25.32±0.03	26.39±0.07	-1.06±0.08
J004402.7+411348	0:44:02.779	41:13:48.34	25.55±0.05	25.22±0.04	0.34±0.06
J004402.9+411224	0:44:02.928	41:12:24.95	25.52±0.04	26.45±0.07	-0.94±0.08
J004402.9+411320	0:44:02.973	41:13:20.86	25.83±0.04	26.37±0.07	-0.54±0.09
J004403.0+411233	0:44:03.096	41:12:33.59	25.52±0.03	26.62±0.09	-1.10±0.09
J004403.2+411137	0:44:03.221	41:11:37.71	24.89±0.02	26.80±0.10	-1.91±0.10
J004403.3+411047	0:44:03.318	41:10:47.98	25.04±0.02	24.76±0.02	0.28±0.03
J004403.3+411050	0:44:03.343	41:10:50.37	25.79±0.05	24.83±0.03	0.96±0.05
J004403.3+411325	0:44:03.341	41:13:25.15	25.38±0.03	26.64±0.08	-1.26±0.09
J004403.4+411328	0:44:03.417	41:13:28.24	25.20±0.02	24.78±0.02	0.42±0.03
J004403.4+411103	0:44:03.435	41:11:03.70	25.75±0.04	27.55±0.19	-1.80±0.19
J004403.4+411307	0:44:03.463	41:13:07.80	26.35±0.07	25.60±0.04	0.75±0.08
J004403.5+411228	0:44:03.558	41:12:28.26	>27.8	26.77±0.10	>1.03
J004403.6+411117	0:44:03.633	41:11:17.31	26.65±0.08	25.80±0.04	0.85±0.09
J004403.7+411339	0:44:03.753	41:13:39.11	24.98±0.03	25.75±0.04	-0.76±0.05
J004403.7+411250	0:44:03.798	41:12:50.84	25.59±0.04	26.80±0.11	-1.21±0.11
J004403.8+411137	0:44:03.811	41:11:37.88	25.55±0.04	25.09±0.03	0.46±0.05
J004403.8+411323	0:44:03.830	41:13:23.03	25.55±0.04	26.45±0.08	-0.90±0.08
J004403.8+411129	0:44:03.864	41:11:29.63	24.70±0.02	25.21±0.03	-0.51±0.03
J004403.9+411357	0:44:03.942	41:13:57.52	26.76±0.11	24.71±0.02	2.06±0.11
J004403.9+411143	0:44:03.982	41:11:43.87	24.40±0.01	25.11±0.03	-0.71±0.03
J004404.0+411353	0:44:04.030	41:13:53.66	22.01±0.00	22.97±0.01	-0.96±0.01
J004404.1+411243	0:44:04.145	41:12:43.12	25.59±0.04	26.67±0.09	-1.09±0.09
J004404.1+411047	0:44:04.154	41:10:47.86	26.32±0.07	25.39±0.03	0.93±0.07
J004404.1+411111	0:44:04.159	41:11:11.29	26.67±0.08	26.04±0.05	0.63±0.09
J004404.1+411152	0:44:04.188	41:11:52.39	26.47±0.08	25.61±0.04	0.86±0.09
J004404.1+411250	0:44:04.197	41:12:50.66	26.40±0.06	25.84±0.04	0.56±0.07
J004404.2+411303	0:44:04.235	41:13:03.54	26.32±0.07	25.52±0.03	0.79±0.07
J004404.2+411235	0:44:04.275	41:12:35.73	25.24±0.03	26.42±0.07	-1.18±0.08
J004404.2+411213	0:44:04.286	41:12:13.63	25.30±0.03	25.63±0.04	-0.34±0.05
J004404.3+411328	0:44:04.319	41:13:28.71	25.33±0.03	24.96±0.02	0.38±0.04
J004404.4+411129	0:44:04.402	41:11:29.44	24.82±0.02	26.29±0.06	-1.47±0.07
J004404.4+411230	0:44:04.480	41:12:30.24	27.17±0.11	25.86±0.04	1.31±0.12
J004404.6+411232	0:44:04.623	41:12:32.38	26.52±0.08	23.87±0.01	2.65±0.08
J004404.6+411100	0:44:04.684	41:11:00.38	27.48±0.14	23.62±0.01	3.86±0.14
J004404.6+411331	0:44:04.687	41:13:31.97	26.24±0.06	25.50±0.04	0.74±0.07
J004404.6+411339	0:44:04.694	41:13:39.76	25.44±0.03	25.87±0.04	-0.43±0.05
J004404.7+411124	0:44:04.714	41:11:24.97	26.33±0.07	25.49±0.04	0.83±0.08
J004404.7+411343	0:44:04.725	41:13:43.86	25.40±0.03	26.47±0.07	-1.07±0.07
J004404.7+411202	0:44:04.778	41:12:02.94	>27.8	25.21±0.03	>2.59
J004404.8+411136	0:44:04.808	41:11:36.46	25.38±0.04	24.89±0.03	0.49±0.04
J004404.9+411130	0:44:04.916	41:11:30.51	25.41±0.03	25.85±0.04	-0.43±0.05
J004404.9+411239	0:44:04.917	41:12:39.40	24.99±0.02	25.79±0.04	-0.79±0.05
J004404.9+411235	0:44:04.930	41:12:35.18	25.27±0.03	25.77±0.04	-0.50±0.05
J004404.9+411321	0:44:04.946	41:13:21.48	24.35±0.01	>27.8	<-3.45
J004404.9+411351	0:44:04.977	41:13:51.91	25.03±0.02	25.26±0.03	-0.23±0.04
J004404.9+411228	0:44:04.991	41:12:28.37	24.32±0.01	24.67±0.02	-0.35±0.02
J004405.1+411329	0:44:05.134	41:13:29.60	27.40±0.17	23.95±0.01	3.44±0.17
J004405.1+411158	0:44:05.149	41:11:58.63	25.38±0.03	25.15±0.03	0.24±0.04
J004405.2+411221	0:44:05.205	41:12:21.37	25.71±0.04	25.11±0.02	0.60±0.04
J004405.2+411341	0:44:05.208	41:13:41.48	26.33±0.08	25.48±0.04	0.85±0.09
J004405.2+411318	0:44:05.272	41:13:18.52	26.03±0.06	25.40±0.03	0.63±0.06

Table 1—Continued

Name (M31ACSV)	R.A. (J2000)	Dec. (J2000)	B_1^a	B_2^b	$B_1 - B_2$
J004405.4+411245	0:44:05.472	41:12:45.25	25.35±0.03	26.07±0.06	-0.73±0.06
J004405.7+411127	0:44:05.756	41:11:27.86	25.45±0.03	26.25±0.07	-0.80±0.08
J004405.7+411049	0:44:05.780	41:10:49.95	24.82±0.02	25.77±0.04	-0.95±0.05
J004405.7+411202	0:44:05.780	41:12:02.58	24.64±0.02	24.13±0.01	0.51±0.02
J004405.8+411049	0:44:05.893	41:10:49.84	25.51±0.03	25.78±0.04	-0.27±0.05
J004405.9+411316	0:44:05.902	41:13:16.97	26.77±0.08	25.64±0.03	1.12±0.08
J004406.0+411348	0:44:06.064	41:13:48.28	>27.8	24.50±0.02	>3.30
J004406.0+411049	0:44:06.073	41:10:49.97	25.81±0.04	26.20±0.06	-0.38±0.08
J004406.1+411235	0:44:06.120	41:12:35.04	23.52±0.01	23.91±0.01	-0.38±0.02
J004406.1+411105	0:44:06.199	41:11:05.71	25.50±0.03	25.24±0.03	0.27±0.04
J004406.2+411354	0:44:06.256	41:13:54.00	25.54±0.03	26.65±0.08	-1.12±0.09
J004406.2+411052	0:44:06.277	41:10:52.21	26.18±0.05	25.62±0.04	0.56±0.06
J004406.3+411305	0:44:06.301	41:13:05.49	26.84±0.10	25.95±0.05	0.88±0.11
J004406.3+411127	0:44:06.307	41:11:27.99	24.65±0.02	25.14±0.03	-0.49±0.03
J004406.3+411223	0:44:06.335	41:12:23.97	25.55±0.03	25.21±0.03	0.34±0.04
J004406.3+411346	0:44:06.367	41:13:46.42	24.75±0.02	25.13±0.03	-0.38±0.03
J004406.3+411238	0:44:06.395	41:12:38.33	24.90±0.02	26.02±0.05	-1.12±0.06
J004406.4+411340	0:44:06.411	41:13:40.76	24.50±0.02	25.83±0.04	-1.33±0.04
J004406.4+411234	0:44:06.418	41:12:34.26	26.89±0.11	>27.8	<-0.91
J004406.4+411404	0:44:06.485	41:14:04.69	26.00±0.05	25.62±0.04	0.38±0.06
J004406.5+411200	0:44:06.545	41:12:00.76	26.32±0.07	25.94±0.05	0.38±0.08
J004406.5+411158	0:44:06.573	41:11:58.46	24.13±0.01	27.25±0.16	-3.12±0.16
J004406.6+411122	0:44:06.606	41:11:22.28	25.23±0.03	24.42±0.02	0.81±0.03
J004406.6+411346	0:44:06.647	41:13:46.98	26.55±0.07	25.85±0.05	0.71±0.09
J004406.6+411342	0:44:06.655	41:13:42.66	>27.8	24.75±0.02	>3.05
J004406.7+411323	0:44:06.736	41:13:23.15	26.06±0.05	25.29±0.03	0.77±0.06
J004406.8+411325	0:44:06.805	41:13:25.34	24.51±0.02	24.33±0.01	0.18±0.02
J004406.8+411224	0:44:06.807	41:12:24.03	25.85±0.04	26.82±0.09	-0.98±0.10
J004406.9+411340	0:44:06.918	41:13:40.04	25.65±0.04	26.64±0.09	-0.99±0.10
J004407.0+411254	0:44:07.022	41:12:54.48	24.15±0.01	25.05±0.03	-0.90±0.03
J004407.0+411146	0:44:07.034	41:11:46.82	24.38±0.01	24.21±0.01	0.17±0.02
J004407.0+411047	0:44:07.067	41:10:47.99	26.70±0.09	25.44±0.03	1.25±0.09
J004407.2+411047	0:44:07.202	41:10:47.64	26.14±0.05	25.58±0.04	0.56±0.06
J004407.2+411354	0:44:07.235	41:13:54.65	25.42±0.04	26.68±0.11	-1.26±0.12
J004407.2+411226	0:44:07.297	41:12:26.00	25.17±0.03	24.92±0.02	0.24±0.03
J004407.3+411300	0:44:07.395	41:13:00.72	25.89±0.04	25.40±0.03	0.49±0.05
J004407.4+411119	0:44:07.400	41:11:19.66	24.78±0.02	27.18±0.13	-2.40±0.13
J004407.4+411204	0:44:07.414	41:12:04.85	24.57±0.02	25.25±0.03	-0.68±0.04
J004407.5+411321	0:44:07.506	41:13:21.46	25.77±0.04	25.32±0.03	0.45±0.05
J004407.5+411350	0:44:07.533	41:13:50.34	25.59±0.03	25.08±0.02	0.50±0.04
J004407.5+411126	0:44:07.561	41:11:26.59	25.54±0.03	26.28±0.06	-0.74±0.06
J004407.5+411304	0:44:07.584	41:13:04.50	25.24±0.03	25.78±0.05	-0.54±0.05
J004407.6+411232	0:44:07.625	41:12:32.91	26.06±0.06	25.55±0.04	0.51±0.07
J004407.6+411238	0:44:07.692	41:12:38.51	25.69±0.04	25.30±0.03	0.40±0.05
J004407.7+411110	0:44:07.721	41:11:10.04	26.18±0.05	25.34±0.03	0.84±0.06
J004407.7+411123	0:44:07.733	41:11:23.74	25.29±0.03	26.04±0.05	-0.75±0.06
J004407.7+411357	0:44:07.764	41:13:57.65	24.94±0.02	23.22±0.01	1.72±0.02
J004407.7+411331	0:44:07.768	41:13:31.48	>27.8	24.58±0.02	>3.22
J004407.7+411333	0:44:07.798	41:13:33.38	25.26±0.03	26.31±0.07	-1.04±0.07
J004407.8+411208	0:44:07.822	41:12:08.62	23.43±0.01	25.58±0.04	-2.15±0.04
J004407.9+411327	0:44:07.930	41:13:27.64	25.10±0.02	24.87±0.02	0.23±0.03
J004408.0+411145	0:44:08.017	41:11:45.58	24.02±0.01	25.36±0.03	-1.34±0.03
J004408.0+411243	0:44:08.049	41:12:43.41	23.28±0.01	22.39±0.01	0.89±0.01
J004408.1+411058	0:44:08.103	41:10:58.51	26.94±0.09	26.37±0.06	0.57±0.11

Table 1—Continued

Name (M31ACSV)	R.A. (J2000)	Dec. (J2000)	B_1^a	B_2^b	$B_1 - B_2$
J004408.1+411302	0:44:08.178	41:13:02.30	25.35±0.03	25.98±0.05	-0.62±0.06
J004408.2+411212	0:44:08.229	41:12:12.03	>27.8	25.11±0.03	>2.69
J004408.3+411202	0:44:08.313	41:12:02.93	26.60±0.09	25.55±0.04	1.04±0.10
J004408.4+411239	0:44:08.438	41:12:39.55	24.80±0.02	24.96±0.03	-0.16±0.03
J004408.4+411347	0:44:08.492	41:13:47.30	21.92±0.00	22.50±0.01	-0.58±0.01
J004408.5+411156	0:44:08.547	41:11:56.42	25.51±0.03	26.68±0.10	-1.17±0.10
J004408.5+411244	0:44:08.597	41:12:44.95	25.12±0.03	24.68±0.02	0.44±0.03
J004408.6+411229	0:44:08.617	41:12:29.70	26.59±0.10	24.66±0.02	1.93±0.10
J004408.6+411236	0:44:08.625	41:12:36.45	25.94±0.05	25.56±0.04	0.37±0.06
J004408.6+411331	0:44:08.653	41:13:31.35	25.67±0.05	>27.8	<-2.13
J004408.6+411106	0:44:08.699	41:11:06.83	25.78±0.04	25.45±0.03	0.33±0.05
J004408.7+411129	0:44:08.738	41:11:29.87	23.76±0.01	24.33±0.01	-0.57±0.02
J004408.7+411319	0:44:08.744	41:13:19.36	25.33±0.03	24.98±0.03	0.36±0.04
J004408.8+411330	0:44:08.830	41:13:30.95	26.03±0.05	27.13±0.12	-1.11±0.13
J004408.8+411235	0:44:08.867	41:12:35.37	27.58±0.17	26.18±0.05	1.40±0.18
J004408.9+411101	0:44:08.907	41:11:01.58	26.21±0.06	25.31±0.03	0.89±0.06
J004408.9+411134	0:44:08.945	41:11:34.73	25.05±0.03	26.34±0.07	-1.29±0.08
J004408.9+411051	0:44:08.953	41:10:51.74	25.54±0.03	25.24±0.02	0.30±0.04
J004409.0+411316	0:44:09.040	41:13:16.80	25.49±0.04	26.51±0.08	-1.02±0.09
J004409.0+411228	0:44:09.094	41:12:28.96	25.00±0.02	25.44±0.03	-0.44±0.04
J004409.1+411119	0:44:09.123	41:11:19.56	24.98±0.02	24.75±0.02	0.23±0.03
J004409.3+411339	0:44:09.307	41:13:39.94	25.63±0.04	26.27±0.06	-0.65±0.07
J004409.3+411226	0:44:09.347	41:12:26.45	25.19±0.03	>27.8	<-2.61
J004409.3+411202	0:44:09.381	41:12:02.61	24.58±0.02	26.11±0.06	-1.53±0.06
J004409.3+411325	0:44:09.393	41:13:25.09	25.58±0.03	26.33±0.06	-0.75±0.07
J004409.4+411311	0:44:09.407	41:13:11.84	>27.8	26.00±0.05	>1.80
J004409.4+411203	0:44:09.418	41:12:03.53	23.99±0.01	26.22±0.06	-2.24±0.06
J004409.4+411247	0:44:09.420	41:12:47.29	24.64±0.02	24.25±0.02	0.38±0.02
J004409.4+411207	0:44:09.446	41:12:07.94	24.68±0.02	26.44±0.08	-1.76±0.08
J004409.5+411147	0:44:09.560	41:11:47.25	26.40±0.06	25.64±0.04	0.76±0.08
J004409.6+411325	0:44:09.682	41:13:25.82	25.94±0.05	26.87±0.12	-0.93±0.13
J004409.7+411243	0:44:09.713	41:12:43.76	24.02±0.01	26.43±0.07	-2.41±0.07
J004409.7+411052	0:44:09.728	41:10:52.24	26.25±0.06	25.03±0.03	1.22±0.07
J004409.7+411115	0:44:09.735	41:11:15.05	25.58±0.03	25.21±0.03	0.37±0.04
J004409.8+411256	0:44:09.832	41:12:56.83	24.28±0.01	26.72±0.09	-2.45±0.09
J004409.9+411108	0:44:09.901	41:11:08.48	26.34±0.06	25.72±0.04	0.62±0.07
J004409.9+411201	0:44:09.910	41:12:01.24	24.58±0.02	26.67±0.09	-2.09±0.09
J004410.0+411213	0:44:10.039	41:12:13.15	26.36±0.06	25.73±0.04	0.63±0.07
J004410.1+411244	0:44:10.182	41:12:44.20	25.64±0.04	25.12±0.03	0.52±0.04
J004410.2+411229	0:44:10.212	41:12:29.35	25.94±0.05	24.92±0.02	1.02±0.05
J004410.2+411258	0:44:10.237	41:12:58.67	26.98±0.12	25.40±0.03	1.58±0.12
J004410.3+411321	0:44:10.309	41:13:21.70	27.79±0.23	23.63±0.01	4.16±0.23
J004410.3+411146	0:44:10.332	41:11:46.91	25.72±0.04	25.17±0.03	0.56±0.04
J004410.3+411052	0:44:10.381	41:10:52.82	26.11±0.05	27.07±0.11	-0.96±0.12
J004410.4+411108	0:44:10.444	41:11:08.31	24.42±0.01	26.01±0.04	-1.59±0.05
J004410.5+411053	0:44:10.503	41:10:53.49	26.00±0.05	25.54±0.03	0.46±0.06
J004410.6+411335	0:44:10.696	41:13:35.66	24.43±0.02	25.96±0.05	-1.54±0.05
J004410.7+411110	0:44:10.714	41:11:10.27	25.40±0.03	26.81±0.10	-1.41±0.10
J004410.9+411107	0:44:10.908	41:11:07.66	25.08±0.03	25.86±0.05	-0.78±0.05
J004410.9+411132	0:44:10.915	41:11:32.53	25.94±0.04	25.56±0.03	0.37±0.05
J004410.9+411104	0:44:10.935	41:11:04.07	24.58±0.02	24.96±0.02	-0.38±0.03
J004411.1+411115	0:44:11.152	41:11:15.72	26.35±0.06	25.76±0.04	0.59±0.07
J004411.1+411228	0:44:11.159	41:12:28.96	25.98±0.04	25.31±0.03	0.66±0.05
J004411.1+411102	0:44:11.182	41:11:02.57	26.77±0.08	26.03±0.04	0.74±0.09

Table 1—Continued

Name (M31ACSV)	R.A. (J2000)	Dec. (J2000)	B_1^a	B_2^b	$B_1 - B_2$
J004411.1+411154	0:44:11.188	41:11:54.73	25.25±0.03	25.09±0.03	0.16±0.04
J004411.2+411056	0:44:11.250	41:10:56.43	26.52±0.08	>27.8	<-1.28
J004411.2+411102	0:44:11.254	41:11:02.99	24.98±0.02	27.48±0.17	-2.50±0.17
J004411.3+411129	0:44:11.397	41:11:29.75	25.19±0.03	25.85±0.04	-0.66±0.05
J004411.4+411116	0:44:11.434	41:11:16.91	25.86±0.04	25.58±0.03	0.28±0.05
J004411.4+411111	0:44:11.446	41:11:11.97	25.61±0.03	25.97±0.05	-0.36±0.06
J004411.5+411154	0:44:11.546	41:11:54.28	27.49±0.14	26.49±0.07	0.99±0.15
J004411.6+411140	0:44:11.639	41:11:40.51	24.64±0.02	26.35±0.07	-1.71±0.07
J004411.6+411228	0:44:11.669	41:12:28.22	25.24±0.03	26.53±0.08	-1.29±0.08
J004411.8+411107	0:44:11.817	41:11:07.49	25.74±0.04	>27.8	<-2.06
J004411.8+411058	0:44:11.822	41:10:58.62	25.47±0.03	25.97±0.05	-0.51±0.06
J004412.0+411204	0:44:12.084	41:12:04.06	24.60±0.02	24.98±0.02	-0.38±0.03
J004412.0+411151	0:44:12.092	41:11:51.38	26.17±0.05	25.73±0.04	0.44±0.07
J004412.1+411137	0:44:12.108	41:11:37.86	27.29±0.12	26.05±0.05	1.24±0.13
J004412.2+411112	0:44:12.219	41:11:12.14	25.63±0.04	25.06±0.02	0.57±0.04
J004412.2+411153	0:44:12.263	41:11:53.71	24.84±0.02	25.07±0.02	-0.23±0.03
J004412.3+411156	0:44:12.343	41:11:56.25	26.63±0.08	26.09±0.05	0.54±0.10
J004412.3+411121	0:44:12.344	41:11:21.19	24.87±0.02	>27.8	<-2.93
J004412.4+411131	0:44:12.405	41:11:31.72	25.74±0.04	26.05±0.05	-0.30±0.06
J004412.4+411318	0:44:12.415	41:13:18.76	24.74±0.02	25.48±0.03	-0.74±0.04
J004412.4+411229	0:44:12.455	41:12:29.15	>27.8	24.64±0.02	>3.16
J004412.5+411058	0:44:12.510	41:10:58.69	24.77±0.02	>27.8	<-3.03
J004412.9+411231	0:44:12.912	41:12:31.43	24.99±0.02	25.60±0.04	-0.61±0.04
J004412.9+411153	0:44:12.957	41:11:53.58	25.21±0.03	25.52±0.03	-0.30±0.04
J004412.9+411152	0:44:12.998	41:11:52.77	25.47±0.03	25.85±0.05	-0.38±0.06
J004413.1+411152	0:44:13.166	41:11:52.45	24.98±0.02	25.53±0.03	-0.55±0.04
J004413.2+411139	0:44:13.264	41:11:39.21	25.28±0.03	26.21±0.06	-0.93±0.07
J004413.3+411308	0:44:13.317	41:13:08.24	24.88±0.02	23.90±0.01	0.98±0.02
J004413.3+411142	0:44:13.374	41:11:42.08	25.94±0.04	27.28±0.15	-1.34±0.16
J004413.5+411204	0:44:13.514	41:12:04.22	24.87±0.02	>27.8	<-2.93
J004413.5+411216	0:44:13.527	41:12:16.09	24.80±0.02	25.27±0.03	-0.47±0.03
J004413.6+411159	0:44:13.689	41:11:59.63	26.00±0.04	>27.8	<-1.80
J004413.8+411143	0:44:13.839	41:11:43.07	24.57±0.02	24.88±0.02	-0.31±0.03
J004414.0+411155	0:44:14.091	41:11:55.09	25.08±0.02	26.64±0.08	-1.56±0.08
J004414.2+411149	0:44:14.219	41:11:49.63	25.97±0.04	25.37±0.03	0.60±0.05
J004414.3+411226	0:44:14.325	41:12:26.56	26.30±0.07	25.50±0.03	0.80±0.08
J004414.3+411218	0:44:14.336	41:12:18.20	23.87±0.01	>27.8	<-3.93
J004415.2+411157	0:44:15.209	41:11:57.32	26.17±0.06	24.40±0.02	1.77±0.06

^aThe $F435W$ VEGAMAG (B -band equivalent) for the first HST observation, taken at UT 21:35, 03-December-2003.

^bThe $F435W$ VEGAMAG (B -band equivalent) for the second HST observation, taken at UT 16:38, 01-March-2004.

Note. — The complete version of this table is in the electronic edition of the Journal. The printed edition contains only a sample.

Table 2. Number of variable stars in the catalog and their photometric properties in each 0.5 magnitude bin.

B_{bright}^a	Number ^b	Mean S/N (σ) ^c	Mean B_{err}^d
21.50 → 22.00	1	268	0.004
22.00 → 22.50	4	239	0.005
22.50 → 23.00	1	193	0.006
23.00 → 23.50	3	134	0.008
23.50 → 24.00	11	102	0.011
24.00 → 24.50	22	76	0.015
24.50 → 25.00	58	56	0.020
25.00 → 25.50	81	40	0.029
25.50 → 26.00	57	30	0.039
26.00 → 26.50	12	20	0.052
26.50 → 27.00	3	13	0.095
27.00 → 27.50	1	9	0.120

^aThe range of magnitudes included in the bin. Only the brighter of the two epochs is included.

^bThe number of variable candidates found whose brighter detection was within the indicated magnitude range.

^cThe mean significance of the detections in this magnitude range in σ .

^dThe mean photometric errors of the detections in this magnitude range in magnitudes.

Table 3. Previously Cataloged Variables

Name (M31ACSV)	Previous Name	Type	Per. (d)	B_{DIR}^a	B_{bright}
J004358.1+411250	[JPN2003] V348	Irregular	23.22 ± 0.01
J004401.0+411132	DIRECT V4569 M31D	Periodic	31.4	21.66	22.13 ± 0.01
J004404.0+411353	DIRECT V5146 M31D	Cepheid	13.523	22.00	22.01 ± 0.00
J004406.6+411122	[JPN 2003] V357	Periodic	132	...	24.42 ± 0.02
J004408.0+411243	DIRECT V5762 M31D	Periodic	56.6	...	22.39 ± 0.01
J004408.4+411347	DIRECT V5816 M31D	Periodic	35.1	21.64	21.92 ± 0.00

^aThe mean B magnitudes (when available) taken from DIRECT (Kaluzny et al. 1999); no B band photometry was available from Joshi et al. (2003).